Solid Colloids with Surface-Mobile DNA Linkers

Stef A. J. van der Meulen* and Mirjam E. Leunissen

FOM Institute AMOLF, Science Park 104, 1098 XG, Amsterdam, The Netherlands

Supporting Information

ABSTRACT: Surface functionalization with bioinspired binding groups is increasingly used to steer nano- and microscale self-assembly processes, with complementary DNA "sticky ends" as one of the most notable examples. The fabrication of well-organized structures is complicated, however, by the sharp association/dissociation transitions and the slow rearrangement kinetics intrinsic to collections of discrete, surface-immobilized binding groups and is aggravated by natural nonuniformities in the surface coating. Here, we demonstrate a novel system of solid microparticles functionalized with specific binding groups—in this case DNA linkers—that are fully mobile along the particle surface. These colloids display qualitatively new behavior and circumvent many of the commonly encountered issues. Importantly, the association/dissociation transition, and thereby the temperature window for equilibrium self-assembly, is much broader. We further find that the linkers are uniformly distributed above the DNA melting temperature, while visibly accumulating at the interparticle contacts below this temperature. The unique combination of binding group mobility with nondeformability, monodispersity, and facile manipulation of solid particles should have a profound impact on DNA-mediated and other bioinspired self-assembly approaches. Moreover, our highly tunable experimental system enables detailed model investigations that will also deepen our fundamental understanding of other systems with surface-mobile binding groups, for instance, biological ligand−receptor interactions.

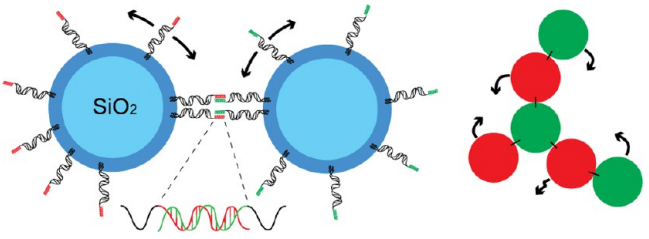

INTRODUCTION

Over the past two decades, the programmability of the behavior of nano/microscale particle suspensions has been dramatically improved, in particular through the use of highly specific noncovalent binding groups that are immobilized on the particle surface. Many of these binding groups are biologically inspired molecular recognition motifs, for instance, taking the form of naturally occurring peptides[1−4] or synthetic DNA "sticky ends".[5−12] The latter are especially promising, because they offer a large variety of user-defined nucleotide sequences and fine thermal control of the binding strength. Using DNA-coated particles, a number of groups recently obtained ordered crystals[8−11] and self-assembled "colloidal molecules".[12] However, the fabrication of such well-organized structures typically requires extensive fine-tuning and annealing of the system. One of the challenges lies in the sharp association/dissociation transition of the particles when one crosses the melting temperature of the DNA linkers.[6,13−17] The temperature window for equilibrium self-assembly thus is easy to miss, leading to "hit and stick" type aggregation without further structural rearrangements. It was also shown that the particles generally have difficulty rolling around each other,[18,19] which may dramatically slow the annealing process, as compared to colloids with a continuous interaction potential, e.g., that of electrostatic origin.[20−22] The intrinsic self-assembly challenges posed by collections of discrete, surface-immobilized binding groups are further aggravated by surface heterogeneities, such as roughness[8] or natural nonuniformities in the coating,[17] as well as unwanted nonspecific interactions. Here, we present a novel system of solid colloids functionalized with specific (DNA) binding groups that are fully mobile along the particle surface, which alleviates many of the aforementioned problems and provides access to profoundly new behavior.

MATERIALS AND METHODS

Particle Functionalization. We functionalized silica microparticles with mobile DNA linkers by first integrating the hydrophobically modified linkers into the lipid bilayer of small unilamellar vesicles (SUVs, Figure 1A). To this end, the phospholipids 1,2-dioleoyl-*sn*-glycero-3-phosphocholine (DOPC, Avanti) and 1,2-dipalmitoyl-*sn*-glycero-3-phosphoethanolamine-*N*-[methoxy(polyethylene glycol)-2000] (DPPE-PEG_{2000}, Avanti) were mixed in 40:1 molar ratio in chloroform. The chloroform was evaporated by a gentle stream of nitrogen and two hours of vacuum desiccation, whereafter the lipids were rehydrated for at least 30 min in 10 mM HEPES/50 mM NaCl (pH 7.4) at a concentration of 2 mg/mL. The lipid mixture was then extruded 21 times through two stacked polycarbonate filters of 30 nm pore size (Avanti). The resulting SUVs were incubated for 15 min with 2−5 μM solutions of cholesterol-conjugated DNA linkers.

We used two different DNA linkers (S and S′, Eurogentec) with 11 base long complementary sticky ends and fluorescently labeled with, respectively, FAM-6 and Cy3 (Figure 1D). The sticky ends were connected to a 47 base pair long double-stranded "backbone" construct with two cholesterol-TEG groups at the opposing end. We prehybridized the backbone by cooling from 90 to 22 °C at a rate of 1.5 °C/min in 10 mM HEPES/150 mM NaCl (pH 7.4) at an overall

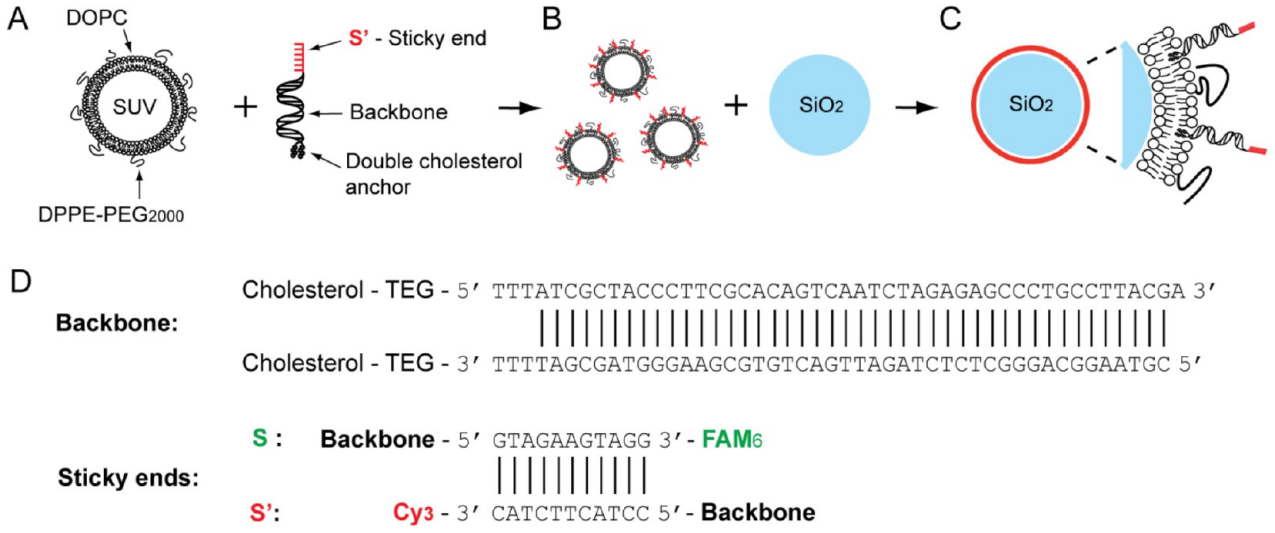

Figure 1. Lipid-bilayer-coated microparticles functionalized with laterally mobile DNA binding groups. Experimental functionalization scheme. DOPC:DPPE-PEG$_{2000}$ SUVs are first mixed with double-cholesterol-conjugated DNA linkers (A) and then with silica microparticles (B), leading to the formation of a DNA-functionalized lipid bilayer that envelopes the particles (C). (D) Base pair sequences of the complementary DNA linkers.

concentration of 5 μM (NanoDrop 2000) and with a 50% excess of the "nonsticky" strand. Surfactant-free suspensions of 0.5 wt % nonporous, nonfunctionalized silica microparticles with a diameter of either 1.30, 2.06 (Microparticles GmbH), or 3.56 μm (Bangs Laboratories) and with coefficients of variability of respectively 2.9, 2.2 and 8.7% were exposed to an equal volume of the DNA-functionalized SUV solution for 15 min at 50 °C (Figure 1B). Excess SUVs were removed by pelletizing (30 s at 50 rcf) and resuspending three times in 10 mM HEPES/50 mM NaCl (pH 7.4). The final linker density on the particles was estimated from the DNA:SUV:particle ratio.

Microscopy Setup and Image Analysis. We used a custom-made sample cell for our various microscopy studies. These sample cells were prepared by cleaning glass coverslips and objective slides by sonication in, subsequently, 2% Hellmanex and Milli-Q. The cleaned coverslips were exposed to UV−ozone for 30 min in a preheated UV−ozone cleaner (ProCleaner). Slivers of coverslips were used as spacers to create three side-by-side channels with a nominal volume of 10 μL each. Slides, spacers, and coverslips were bonded together with optical adhesive (NOA68, Norland), which was also used to seal the channels. Fluids could still be exchanged through 1 mm diameter predrilled holes in the objective slides. The channels were first passivated for 30 min with 5 mg/mL casein solution (casein sodium salt from bovine milk, Sigma Aldrich), after which the channels were rinsed with copious amounts of 10 mM HEPES/50 mM NaCl (pH 7.4).The DNA-functionalized particle suspensions were then administered to the channels, where they sedimented to effectively form a two-dimensional system. The channels were oriented such that the particles sedimented to the surface of the coverslip, which facilitated bright-field, confocal, and TIRF microscopy. For our quantitative association/dissociation studies, the sample cells were mounted on a custom-made stage setup on a Nikon Eclipse Ti-E light microscope, which enabled fine temperature control while imaging in transmission mode. At each temperature of interest we recorded five independent images and determined the singlet fraction by common video microscopy methods. Our analysis method did not distinguish between pairs of bound particles and singlets that just happened to be very near each other in our still images. We corrected for this systematic error with a simple 2D simulation of "hard spheres" at the same overall concentration as the experiment.

RESULTS AND DISCUSSION

Particle Functionalization. We created a system of solid particles with surface-mobile binding groups by coating silica microspheres with a fluid lipid bilayer and hydrophobically anchored DNA linkers (Figure 1A and Materials and Methods). The single-stranded complementary DNA sticky ends (S and S′) were fluorescently labeled and were connected to a ∼16 nm long double-stranded backbone construct with two cholesterol groups at the opposing end (Figure 1D). The hydrophobic cholesterol anchors inserted spontaneously into the lipid bilayers of a preformed suspension of small unilamellar vesicles (SUV), leaving the sticky ends pointing outward. Subsequently, a process of vesicle rupture and fusion[23,24] led to the formation of a uniform DNA-functionalized lipid bilayer around the silica microparticles. We verified the stability of the double-cholesterol anchoring of the linkers in the temperature range used for our microscopy studies with quartz crystal microbalance (QCM-D) measurements on solid supported lipid bilayers of similar composition as those on the particles (Figure S1 and methods within the Supporting Information). In these measurements, we first let the DNA linkers adsorb to the lipid bilayer and then tried to desorb them again by prolonged rinsing with pure buffer. In agreement with the earlier results of Pfeiffer et al.,[25] we found that the second cholesterol group greatly strengthens the coupling to the lipid bilayer, as compared to a single cholesterol anchor, and makes the linker attachment essentially irreversible. Importantly, the DNA-functionalized lipid bilayer largely determines the particle interactions, independent of the material of the particle core. To further suppress the unwanted nonspecific interactions that frequently plague colloid science, we introduced some additional short-ranged steric repulsion by including a small amount of PEG-ylated lipids (Flory radius ∼3.8 nm), analogous to common practices for giant unilameller vesicles. Although the PEG-ylated lipids are mobile, their expulsion from the interparticle contact zone is counteracted by the lateral osmotic pressure of the PEG-ylated lipid reservoir on the rest of the particle. The resulting PEG distribution provides the steric repulsion and, as a result, we found that in suspensions of a single particle type (S or S′ functionalized) most beads were stably dispersed as singlets.

Binding Group Mobility. A crucial aspect of our new colloidal system is the lateral mobility of the cholesterol-

anchored DNA linkers along the lipid-coated particle surface. The main phospholipid component is DOPC, which has a melting point of −20 °C. The lipid bilayer around the microparticles should thus be in the liquid phase and the DNA linkers should diffuse around freely, while remaining anchored to the particles. To probe the mobility of the DNA linkers, we conducted comparative fluorescence recovery after photobleaching (FRAP) studies. Lipid-coated microparticles functionalized with fluorescently labeled S′ DNA linkers were made to stick to the bottom of a nonpassivated sample cell. We then bleached them on one side with a 500 ms high-intensity laser pulse (λ_{ex} = 561 nm), while the fluorescence emission was monitored in TIRF mode (Figure 2). The partial recovery of

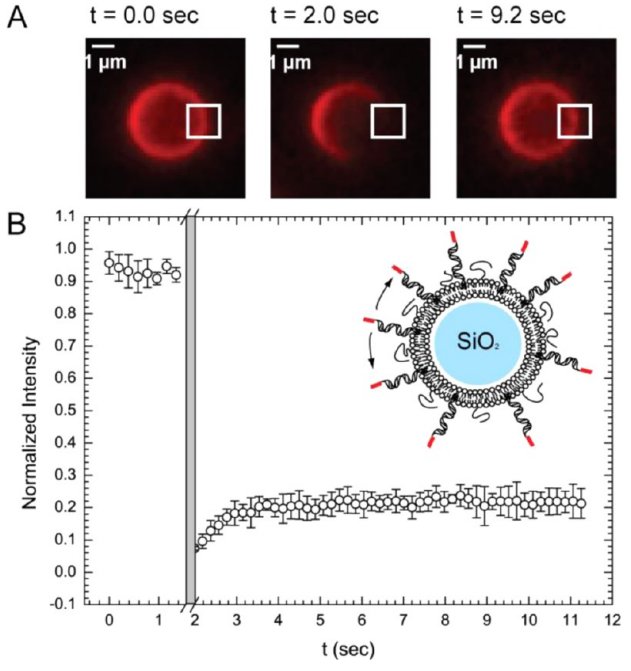

Figure 2. FRAP measurement of the lateral mobility of the lipid-bilayer-anchored DNA linkers on the particles. (A) Fluorescent micrographs of the emission of Cy3-labeled DNA linkers on a 3.56 μm diameter particle, before and after a partial bleach at t = 2.0 s (shaded bar in B). (B) Plot of the normalized mean pixel intensity of the bleached area (white square in A) versus time. The error bars represent the standard deviation in the averaged measurements of five particles.

the fluorescence signal from the bleached area proves that the DNA linkers are indeed mobile, as unbleached and bleached linkers redistribute around the particle. The fluorescence intensity does not return to the initial prebleach level, because the irreversible bleaching of the DNA linkers on a major part of the particle effectively dilutes the overall dye concentration. The time scale of the recovery is on the same order of magnitude as what was found by Gopalakrishnan et al.,[26] who probed the diffusivity of fluorescently labeled lipids in bilayers on silica particles.

The unique combination of binding group mobility with the monodispersity and nondeformability of solid colloids bridges the existing gap between hard nano/microparticles with (covalently coupled) immobile binding groups and soft, "floppy" objects with mobile binding groups. Examples of the latter are DNA-functionalized lipid vesicles[27−29] and possibly oil-in-water droplets,[30] which both experience a strong deformation of their contact zone upon bond formation (for the oil droplets it is not known, however, whether the DNA linkers are actually mobile). Importantly, the pronounced surface-mobility of the DNA linkers in our system also implies that their distribution around individual particles is intrinsically uniform, without requiring any special efforts during the particle functionalization, something that is not necessarily true for the coupling of immobile binding groups.

Mobile-DNA-Mediated Interactions. We studied the association/dissociation behavior of our mobile-DNA-coated colloids by mixing equal amounts of S- and S′-functionalized 1.30 μm diameter particles in a passivated sample cell (see Materials and Methods). At 25 °C the particles formed extensive clusters, which dissociated when the temperature was raised to 55 °C (Figure 3A−D). The dissociation into individual particles is clearly demonstrated by the time-averaged micrographs, in which the highly mobile singlets have a blurry appearance, while the less mobile particles inside clusters remain clearly distinguishable. This temperature-dependent association/dissociation behavior could be cycled back and forth many times. The clusters that formed at low temperature displayed an alternating order of the red- and green-fluorescent-labeled complementary particles (Figure 3C). The specificity and the temperature-dependence of the interactions indicate that these are indeed mediated by the reversible hybridization of the complementary DNA linkers and that unwanted nonspecific interactions are suppressed.

In the confocal micrograph of Figure 3C, one can also see that the contact points between the complementary particles inside clusters appear brighter, in this case with a yellow color due to overlap of the red and green fluorescent signals. Interestingly, in a system of S- and S′-functionalized 3.56 μm diameter particles that were randomly jammed together at a density where all translational freedom of the particles was eliminated—so that they also stayed in contact at elevated temperatures, independent of the state of DNA linker binding—the bright spots only appeared at low temperature and were absent at 55 °C (Figure 3E,F). To verify that this was not an imaging artifact due to the overlapping signals from the two fluorescence channels, we performed experiments with complementary particle mixtures in which only one of the DNA linker types (S) was fluorescently labeled [Figures 4 and S2 (Supporting Information)]. Also in these experiments we observed a nonuniform distribution of the fluorescence intensity around the particles at 25 °C, with the more intense fluorescent spots of the S linkers coinciding with the contact points between complementary particles. Apparently, the DNA linkers distribute uniformly around the particles above the sticky end melting temperature (Figure 3F), but they collect in the interparticle contact zones upon bond formation below this temperature (Figure 3E and Figure 4), a direct and remarkable consequence of the surface mobility of the binding groups.

Association/Dissociation Transition. We quantified the association/dissociation behavior by recording the fraction of unbound particles, or "singlet fraction", as a function of the temperature for four different DNA linker densities on 1.30 μm diameter particles (Figure 5 and Materials and Methods). We let 1:1 mixtures of the S- and S′-functionalized particles associate for 15 min at 30 °C and then increased the temperature to 60 °C in steps of 2 °C, with a 15 min waiting time per step. We used these 15 min equilibration intervals to ensure that at the start of the measurement all particles were clustered and to avoid possible kinetic effects due to

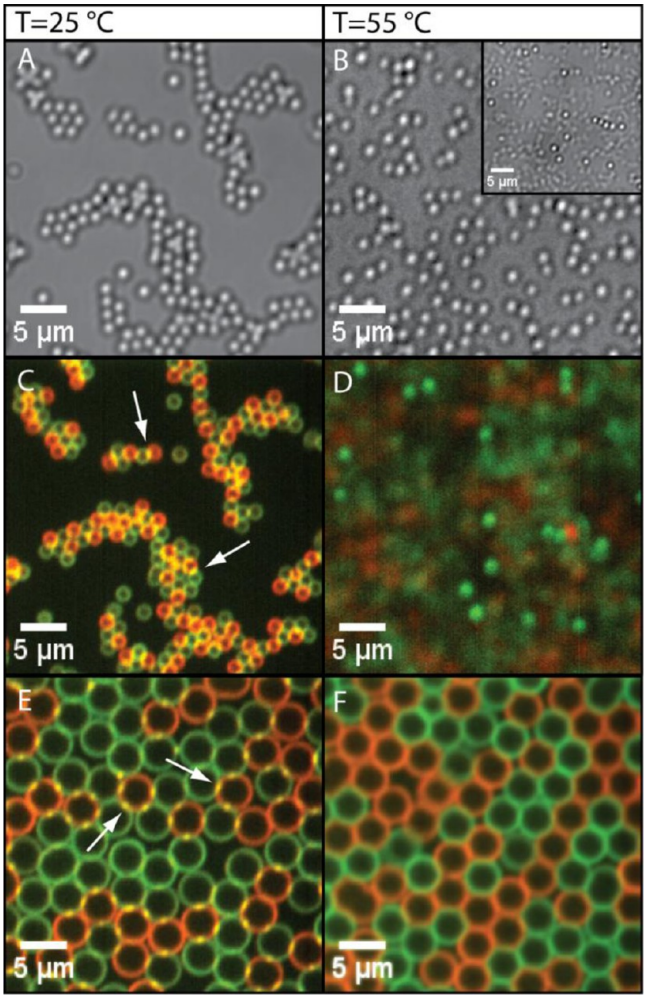

Figure 3. Temperature-dependent behavior of 1:1 microparticle mixtures functionalized with complementary mobile DNA linkers. (A, B) Bright-field snapshots of freely suspended 1.30 μm diameter S- and S′-functionalized particles at 25 °C (A) and 55 °C (B). The inset is a time average of 100 frames. (C and D) Time averages of 100 confocal micrographs corresponding to panels A and B, with S shown in green and S′ in red. (E and F) Time averages of 100 confocal images at 25 °C (E) and 55 °C (F) of a high-density fully jammed random packing of 3.56 μm diameter particles with no remaining translational freedom to self-organize or diffuse away (the field of view drifted somewhat between the low- and high-temperature recordings, though). The white arrows in panels C and E indicate examples of the bright fluorescent spots that appear at low temperature at the complementary particle contacts, due to a locally enhanced linker concentration. The occasional bright spot between two particles of the same color is the result of a small number of fluorescent DNA-functionalized SUVs from our particle preparation procedure having been left behind in the suspension.

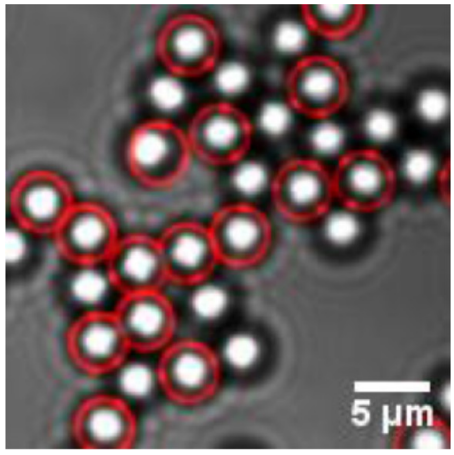

Figure 4. Single-dye fluorescence intensity increase at the contact points between particles carrying complementary mobile DNA linkers. Composite image of 100 time-averaged bright-field snapshots (in gray) and 100 time-averaged confocal fluorescence snapshots (in red) of 3.56 μm diameter S- and S′-functionalized particles interacting with each other at 25 °C. Only the S linkers were fluorescently labeled and appear as red shells around their host particles, while the S′-functionalized particles are only visible in bright-field mode. The separate bright-field and fluorescence images are shown in the Supporting Information (Figure S2).

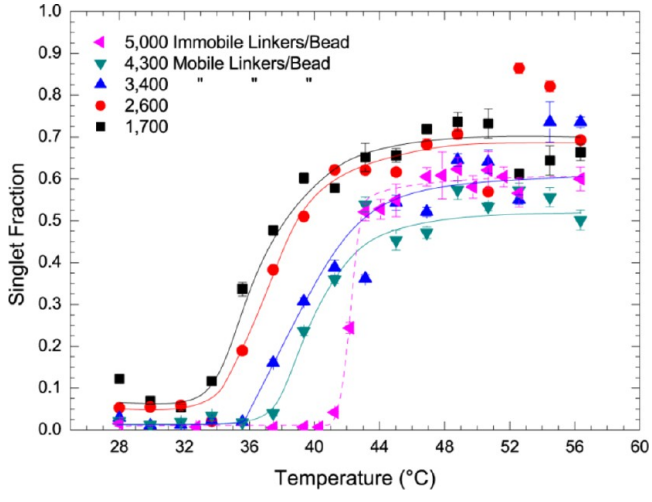

Figure 5. Temperature-induced dissociation transition for microparticles with different DNA linker densities. Shown is the particle singlet fraction as a function of the temperature in 1:1 mixtures of 1.30 μm diameter particles with mobile S and S′ linkers (solid lines) and of 1.05 μm diameter Dynabeads with immobile S and S′ linkers (dashed line). The lines are drawn as a guide to the eye. The error bars represent the standard deviation from five independent images at each temperature.

redistribution of the linkers on the particle surface. The equilibrium linker distribution depends on a combination of factors, including the number of contacts with neighboring particles, and nonequilibrium effects could occur if the speed of linker redistribution is slow compared to other relevant processes in the system. From our FRAP measurements we find that linker diffusion takes on the order of seconds/μm^2. This should be compared with a heating rate of minutes/°C and the characteristic association time of the particles. The latter depends on the particle concentration and size (through their diffusivity) and is on the order of several tens of seconds for micrometer-sized particles. Our experimental system thus had ample time to reach equilibrium in each temperature step, which is also confirmed by the fact that faster ramps of 1 °C/min gave essentially the same results.

As expected for DNA-mediated particle interactions, the dissociation curves in Figure 5 systematically shift to lower temperatures as the mobile linker density decreases, thus demonstrating good control over the particle functionalization and their association behavior. There is an important difference with the dissociation curves of particles with immobile linkers, though. To illustrate this, we performed a similar experiment

with 1.05 μm diameter Dynabeads (MyOne Streptavidin C1, Molecular Probes), functionalized with the same sticky ends through a surface-immobile biotin−streptavidin coupling, as described before.[15,31] From Figure 5, it is clear that at similar overall linker densities on the particles, the dissociation transitions of our mobile-DNA-coated colloids are much broader (width 6.5 ± 1.7 °C) than the transitions observed for the immobile-DNA-coated particles, which are extremely sharp (~1−2 °C, as is usual for these linker densities[15]). A detailed comparison with the more elaborate immobile-DNA-coated colloid data of Wu et al.[32] leads to the same conclusion. Assuming an interparticle binding distance of roughly the DNA linker length,[17] it follows from geometrical considerations that at our lowest and highest mobile linker densities (1700 and 4300 linkers/bead) there are, respectively, about 12 and 30 linkers in the contact zone within reach of the linkers on the partner particle, that is, if we neglect the accumulation of linkers in the contact zone upon bond formation (Figure 3E). These lower-limit estimates roughly correspond to immobile-DNA-coated colloid systems with sticky end fractions $\chi = 0.1-0.15$ in ref 32. There it was found that the transition width is 1.5 °C for $\chi = 0.1$ and 1.2 °C for $\chi = 0.2$, with even sharper transitions as the number of linkers in the contact zone increases further. Due to the somewhat different buffer conditions (73 versus 50 mM NaCl in our experiments) we cannot directly compare the dissociation temperature at 50% singlets (T_m), but the strongly different width of the curves does support the conclusion that the broad transitions are a distinctive property of our mobile-DNA-coated colloids. A couple of theoretical studies on other types of systems also suggest that binding group (im)mobility leads to qualitatively different equilibrium interactions,[33,34] but a simple conceptual understanding of the broad transitions is still lacking. It is important to realize, though, that the equilibrium interactions are no less predictable or user-tunable for particles with mobile binding groups than they are for immobile binding groups. One only needs to account for the fact that the equilibrium distribution of mobile linkers is not strictly uniform but the direct result of other system parameters that could be included in an appropriate model (for instance, building on the analytical theories of refs 35 and 36).

The less dramatic dissociation transition that we observe for our mobile-DNA-coated colloids provides a much larger temperature window for equilibrium self-assembly and should thus facilitate the formation of well-organized structures. Moreover, even if we cool quickly to temperatures below the equilibrium self-assembly window—where the bonds are very strong—we find that the mobile-DNA-coated particle clusters are much more compact and ordered than the typically fractal-like low-temperature aggregates of immobile-DNA-coated colloids, as is exemplified by an increase of the average number of nearest neighbors from 2.6 ± 1.0 to 3.4 ± 1.2 in parts A and B of Figure 6, respectively. Ramping the temperature down more slowly, from 52 to 25 °C in 3 h, still gives slightly better structures, raising the average number of nearest neighbors to 4.2 ± 1.3 (Figure 6C), but even without any fine-tuning or annealing one can get good self-organization results. It is noteworthy that when the temperature is increased, the clusters of mobile-DNA-coated particles develop a "floppy" character while the particles are still connected, instead of "shattering" in a sudden transition from a tightly bound to a fully unbound state the way immobile-DNA-coated colloids do (compare Supplementary Movies S1 and S2, Supporting Information). We speculate that these observations are due to a collective mobility of the bonds in the contact zone that allows particles to more easily roll around each other and rearrange, besides the mobility of individual linkers when they are not bound.

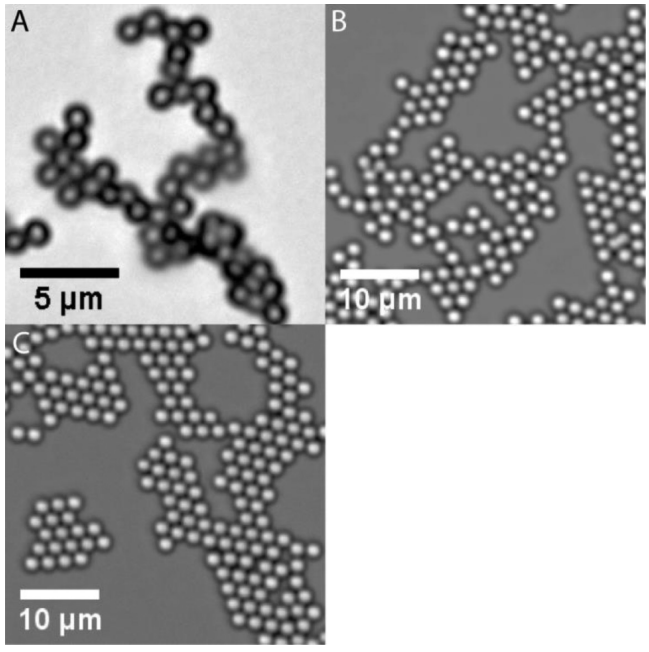

Figure 6. Self-organization of complementary microparticle mixtures functionalized with either immobile or mobile DNA linkers. 1:1 mixtures of S- and S′-functionalized particles were cooled quickly from a fully dissociated state at 52 °C to a fully associated state at 25 °C in 15 min. The bright-field snapshots show the resulting structures for (A) 1.0 μm diameter particles with immobile DNA linkers and (B) 2.0 μm diameter particles with mobile DNA linkers. (C) The same sample as in panel B after redissociating and slowly cooling from 52 to 25 °C in 3 h.

CONCLUSION

We have demonstrated a novel system of hard, nondeformable particles that interact specifically and reversibly through DNA binding groups that are fully mobile along the particle surface. These colloids display qualitatively new behavior, including a much broader association/dissociation transition than is common for colloids with immobile binding groups. The observed accumulation of linkers at the interparticle contacts suggests that the binding group mobility could also enable other types of new behavior, for instance in the form of "self-limited" association processes.[37−40] And, whereas the current focus mostly was on equilibrated systems, one could also obtain time-dependent properties that depend on the flux of binding groups along the particle surface. This could be done by tuning the different time scales in the system, in particular through the particle size, the linker coverage, and the rate of temperature change. The facile manipulation of the solid particles and the temperature-tunable binding strength of the easy-to-image fluorescent DNA linkers enable detailed quantitative investigations. Moreover, the particle functionalization uses no harsh coupling chemistries and requires only commercially available components, and the DNA linkers could even be used to attach other types of binding groups. We therefore expect this new model system to be broadly applicable and to deepen our fundamental understanding of a range of bioinspired self-assembly approaches and of other systems with surface-mobile

binding groups, for instance, biological ligand−receptor interactions.

■ ASSOCIATED CONTENT

Supporting Information

Experimental procedures for the QCM-D measurements and Figures S1 and S2 and Movies S1 and S2. This material is available free of charge via the Internet at http://pubs.acs.org.

■ AUTHOR INFORMATION

Corresponding Author

meulen@amolf.nl

Notes

The authors declare no competing financial interest.

■ ACKNOWLEDGMENTS

We thank Ralf P. Richter and Galina V. Dubacheva for facilitating and collaborating on the QCM-D measurements, the group of Daan Frenkel—especially Bortolo M. Mognetti and Patrick Varilly—for useful discussions, the AMOLF technical support for equipping our microscope setup with temperature control functionality, and Huib J. Bakker for a critical reading of the manuscript. This work was supported by the research program of the Foundation for Fundamental Research on Matter (FOM), which is part of The Netherlands Organization for Scientific Research (NWO).

■ REFERENCES

(1) Lee, S.-K.; Maye, M. M.; Zhang, Y.-B.; Gang, O.; van der Lelie, D. *Langmuir* **2009**, *25*, 657−60.

(2) Hiddessen, A. L.; Rodgers, S. D.; Weitz, D. A.; Hammer, D. A. *Langmuir* **2000**, *16*, 9744−9753.

(3) Mann, S.; Shenton, W.; Li, M.; Connolly, S.; Fitzmaurice, D. *Adv. Mater.* **2000**, *12*, 147−150.

(4) Schoen, A. P.; Hommersom, B.; Heilshorn, S. C.; Leunissen, M. E. *Soft Matter* **2013**, *9*, 6781−6785.

(5) Alivisatos, A. P.; Johnsson, K. P.; Peng, X.; Wilson, T. E.; Loweth, C. J.; Bruchez, M. P.; Schultz, P. G. *Nature* **1996**, *382*, 609−611.

(6) Mirkin, C. A.; Letsinger, R. L.; Mucic, R. C.; Storhoff, J. J. *Nature* **1996**, *382*, 607−609.

(7) Geerts, N.; Eiser, E. *Soft Matter* **2010**, *6*, 4647.

(8) Kim, A. J.; Biancaniello, P. L.; Crocker, J. C. *Langmuir* **2006**, *22*, 1991−2001.

(9) Nykypanchuk, D.; Maye, M. M.; van der Lelie, D.; Gang, O. *Nature* **2008**, *451*, 549−52.

(10) Macfarlane, R. J.; Lee, B.; Jones, M. R.; Harris, N.; Schatz, G. C.; Mirkin, C. a *Science (New York, N.Y.)* **2011**, *334*, 204−8.

(11) Casey, M. T.; Scarlett, R. T.; Benjamin Rogers, W.; Jenkins, I.; Sinno, T.; Crocker, J. C. *Nat. Commun.* **2012**, *3*, 1209.

(12) Wang, Y.; Breed, D.; Manoharan, V.; Feng, L.; Hollingsworth, A.; Weck, M.; Pine, D. *Nature* **2012**, *490*, 51−55.

(13) Jin, R.; Wu, G.; Li, Z.; Mirkin, C. A.; Schatz, G. C. *J. Am. Chem. Soc.* **2003**, *125*, 1643−1654.

(14) Lukatsky, D.; Frenkel, D. *Phys. Rev. Lett.* **2004**, *92*, 1−4.

(15) Dreyfus, R.; Leunissen, M.; Sha, R.; Tkachenko, A.; Seeman, N.; Pine, D.; Chaikin, P. *Phys. Rev. Lett.* **2009**, *102*, 5−8.

(16) Leunissen, M. E.; Dreyfus, R.; Sha, R.; Seeman, N. C.; Chaikin, P. M. *J. Am. Chem. Soc.* **2010**, *132*, 1903−13.

(17) Leunissen, M. E.; Frenkel, D. *J. Chem. Physics* **2011**, *134*, 084702.

(18) Licata, N. A.; Tkachenko, A. V. *EPL* **2008**, *81*, 48009.

(19) Xu, Q.; Feng, L.; Sha, R.; Seeman, N.; Chaikin, P. *Phys. Rev. Lett.* **2011**, *106*, 5−8.

(20) Leunissen, M. E.; Christova, C. G.; Hynninen, A.-P.; Royall, C. P.; Campbell, A. I.; Imhof, A.; Dijkstra, M.; van Roij, R.; van Blaaderen, A. *Nature* **2005**, *437*, 235−40.

(21) Bartlett, P.; Campbell, A. *Phys. Rev. Lett.* **2005**, *95*, 128302.

(22) Shevchenko, E. V; Talapin, D. V; Kotov, N. A; O'Brien, S.; Murray, C. B. *Nature* **2006**, *439*, 55−9.

(23) Baksh, M. M.; Jaros, M.; Groves, J. T. *Nature* **2004**, *427*, 139−41.

(24) Kong, Y.; Parthasarathy, R. *Soft Matter* **2009**, *5*, 2027.

(25) Pfeiffer, I.; Höök, F. *J. Am. Chem. Soc.* **2004**, *126*, 10224−10225.

(26) Gopalakrishnan, G.; Rouiller, I.; Colman, D. R.; Lennox, R. B. *Langmuir* **2009**, *25*, 5455−8.

(27) Benkoski, J.; Höök, F. *J. Phys. Chem. B* **2005**, *109*, 9773−9779.

(28) Chan, Y.-H. M.; Lenz, P.; Boxer, S. G. *Proc. Natl. Acad. Sci. U. S. A.* **2007**, *104*, 18913−8.

(29) Beales, P. A.; Vanderlick, T. K. *J. Phys. Chem. A* **2007**, *111*, 12372−12380.

(30) Hadorn, M.; Boenzli, E.; Sørensen, K. T.; Fellermann, H.; Eggenberger Hotz, P.; Hanczyc, M. M. *Proc. Natl. Acad. Sci. U. S. A.* **2012**, *109*, 1−6.

(31) Dreyfus, R.; Leunissen, M. E.; Sha, R.; Tkachenko, A.; Seeman, N. C.; Pine, D. J.; Chaikin, P. M. *Phys. Rev. E* **2010**, *81*, 1−10.

(32) Wu, K.-T.; Feng, L.; Sha, R.; Dreyfus, R.; Grosberg, A. Y.; Seeman, N. C.; Chaikin, P. M. *Proc. Natl. Acad. Sci. U. S. A.* **2012**, *109*, 18731−18736.

(33) Manghi, M.; Aubouy, M. *Eur. Phys. J.. E* **2003**, *11*, 243−54.

(34) Zhang, C.-Z.; Wang, Z.-G. *Langmuir* **2007**, *23*, 13024−39.

(35) Varilly, P.; Angioletti-Uberti, S.; Mognetti, B. M.; Frenkel, D. *J. Chem. Phys.* **2012**, *137*, 094108.

(36) Angioletti-Uberti, S.; Varilly, P.; Mognetti, B. M.; Tkachenko, A. V; Frenkel, D. *J. Chem. Phys.* **2013**, *138*, 021102.

(37) Kisak, E.; Kennedy, M. *Langmuir* **2000**, *16*, 2825−2831.

(38) Effenterre, D. Van; Roux, D. *EPL* **2007**, 543.

(39) Martinez-Veracoechea, F.; Leunissen, M. *Soft Matter* **2013**, *9*, 3213−3219.

(40) Vial, S.; Nykypanchuk, D.; Yager, K.; Tkachenko, A. V.; Gang, O. *ACS Nano* **2013**, *7*, 5437−5445.